

Analytical approach and experimental studies of 3D behavior textile composite with carbon reinforcement of the interlock 2.5D type

Christiane EL HAGE¹, Zoheir ABOURA², Rafic YOUNES³

Malk L. BENZEGGAGH¹, Mohamad ZOAETER³

¹Université de Technologie de Compiègne. Laboratoire de Roberval de Mécanique.
B.P 20529 F- 60205 Compiègne Cedex

email: elhagechristiane@hotmail.com, benzeggag@utc.fr

²L3M IUT de Tremblay en France Paris 8. Rue de la Râperie 93290 Tremblay-en-France
email: aboura@utc.fr

³Université Libanaise - Faculté de Génie, Equipe de recherche E2M.
email: ryounes@ul.edu.lb, zoaeter@ul.edu.lb

Abstract

The purpose of this paper is to present three-dimensional analytical model, for the prediction of the mechanical properties concerning the interlock CFRP, taking into account their structural parameters. The 3D mechanical behavior was first studied. The strong anisotropy of these materials makes the REV difficult to be identified. Three REV are proposed for three transversal sections with different internal geometrical design. For each REV, the three-dimensional elastic properties represented by the 9 constants of engineer and the matrices of rigidity are given analytically. Moreover the analytical model is extended to predict the ultimate properties of failure by using the tensorial criterion 3D of Tsai. The results from these modeling are compared with experimental results under tensile loading followed in real time by the measurement of signals acoustic emission performed during the tests. Damages and failure mechanisms are identified by microscopic observation and compared by their identification attributed to stages of amplitude.

Keywords: Interlock, Homogenization, Unit cell, 3D Failure criteria, Acoustic emission

1. Introduction

The three-dimensional woven composite materials are the subject of multitude researches developed under the impulse of aerospace and automobile industries. Multidirectional weavings were developed to manufacture composite structures with high performances. Generally, a composite weaving material depends mainly on the nature of the components, the rate of reinforcement and the type of weaving. Moreover the reinforcement in the third direction allows a clear improvement of the interlaminar resistance which remains one of the principal concerns, with respect to the laminated composite materials (Aboura et al., 1995). An example of a composite of weaving angle interlock 2.5D, reinforced by carbon fibers, T300J/RTM6 Epoxy, has been investigated in this study. The structure of interlock 2.5D is formed by undulation yarns in the directions of weft and fill, thus reinforcing its third direction. In the first part of this work, the mechanical behavior and the ultimate failure of angle interlock were investigated under tension load. To improve the mechanical properties of weaving angle interlock, a close attention is paid to internal architectural design details of angle interlock CFRP. Modeling the mechanical compartment of three dimension fabric composite, impose to modeling the geometrical internal structure with less complexity. Or, the 3D fabric composite has an anisotropic structure. In this case, it's necessary to homogenize this type of materials, by identifying a representative elementary volume (REV). The strong anisotropy of these materials makes the REV difficult to be identified. We proposed in this study, three REV, for three transversal sections. For each REV, the 3D mechanical properties are determined by an analytical homogenization model, based on the sum of average rigidities and volumes of components. This analytical model is inspired by the work of (Scida et al., 1998) applied to woven 2D for predicting the three dimensional elastic properties. For 3D composite fabric, this model is applied to weaving 3D orthogonal in the work of (El Hage et al., 2005), (Aboura et al., 2005). It allows the prediction of the mechanical properties by taking into account structural parameters (mechanical properties of the components and geometrical properties of internal architecture). It comes out from this model the three-dimensional elastic properties represented by the 9 constants of engineer, the stiffness matrix, as well as the prediction of the ultimate properties of failure by the application of the tensorial criterion 3D of Tsai. The effect of internal geometrical details has been highlighted by comparing the results of these modeling with experimental results. In the second part of this study, the damage and the rupture processes were identified by optical microscopy. The acoustic emission, a non destructive evolution, was performed during the mechanical tensile test. Acoustic emission (AE) waveform parameters were investigated as damage indicators and related to the physical

damage process. A correlation between the AE waveform parameters and the damage identified by optical microscopic was then proposed.

2. Presentation of materials and choice of REV

The materials consist by perform of a carbon fiber T300J-Toray, placed inside a mould and then injected by resin (M6) according to the process of Resin Transfert Molding (RTM). The internal design of this angle interlock CFR investigated in this study has been visualized by macroscopic studies obtained by electronic microscopic swiping (JOEL-JSM 6100 Scanning Microscope, EMB). The thickness is 8mm. This composite is fabricated by seventeen yarns distributed in each direction weft and fill. The figure 1a is a longitudinal section in the weft direction. We visualize the waft yarns and the sections of filler yarns. The sections of filler yarns are closely aligned in the horizontal and vertical directions. The warp yarns intercept the filler yarns in three consecutive levels. The figure 1b is a transversal section. We observed the weaving filler yarns and the sections of warp yarns. Two successive planes constitute this type of interlock babric. By vertical plane, the warp yarns are intercalated by two planes of filler yarns. The figure 2 shows by transparency, the two planes which are repeated along the transversal direction. An elementary representative volume is selected to be the smallest volume; while by multiplying in the three directions of space, it constitutes the total material. The required mechanical properties of REV are the same for the global composite. The research of REV is based on microscopic studies. The strong anisotropy of these materials makes it difficult for the choice of REV. In figure 1, the REV is presented by a rectangle drawn with a discontinued line in both longitudinal and transversal section. In the longitudinal section of REV, the distribution of warp yarns and filler yarns is sensibly put in order. On the other hand, in the cross section of REV, warp yarns represented by their sections, are intercalated by ply in vertical and horizontal direction.

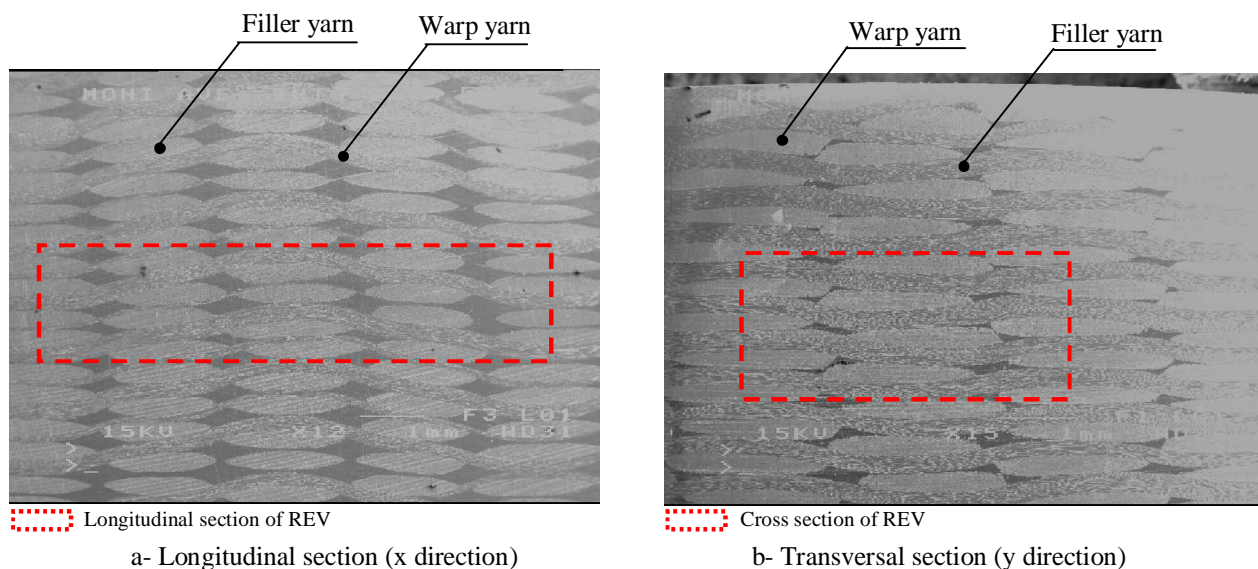


Figure 1: Internal design of angle interlock 2.5D fabric, obtained by EMB

3. Geometrical modeling of REV

For modeling studies, it's recommended as possible, to propose a geometrical modeling of REV which has the less complex internal geometrical structure. In the studies on orthogonal 3D fabric realized by (El Hage et al., 2005), the choice of REV (GC) taking into account the details of vertical curves, predicted better the ultimate properties with respect to experimental studies. So, to highlighting the effect of choice of geometrical modeling of REV of angle interlock (CFRP) on the ultimate properties, we proposed in this study three REV. All these REV have the same geometrical modeling to the longitudinal section. But, to the transversal section, we proposed one geometrical modeling for each REV.

3.1. Modeling of longitudinal section of REV

In longitudinal section of each REV, the staircase model is proposed in this study to model the warp yarn. The staircase model, represent the combination of undulate and linear equations. The cross section of filler yarns are aligned in two directions, fill direction (x) and z direction. In respect to the profile of warp yarn modeled by a staircase geometrical model, the cross section of filler yarn is modeled by the sum of rectangle and two half of ellipse (Figure 2).

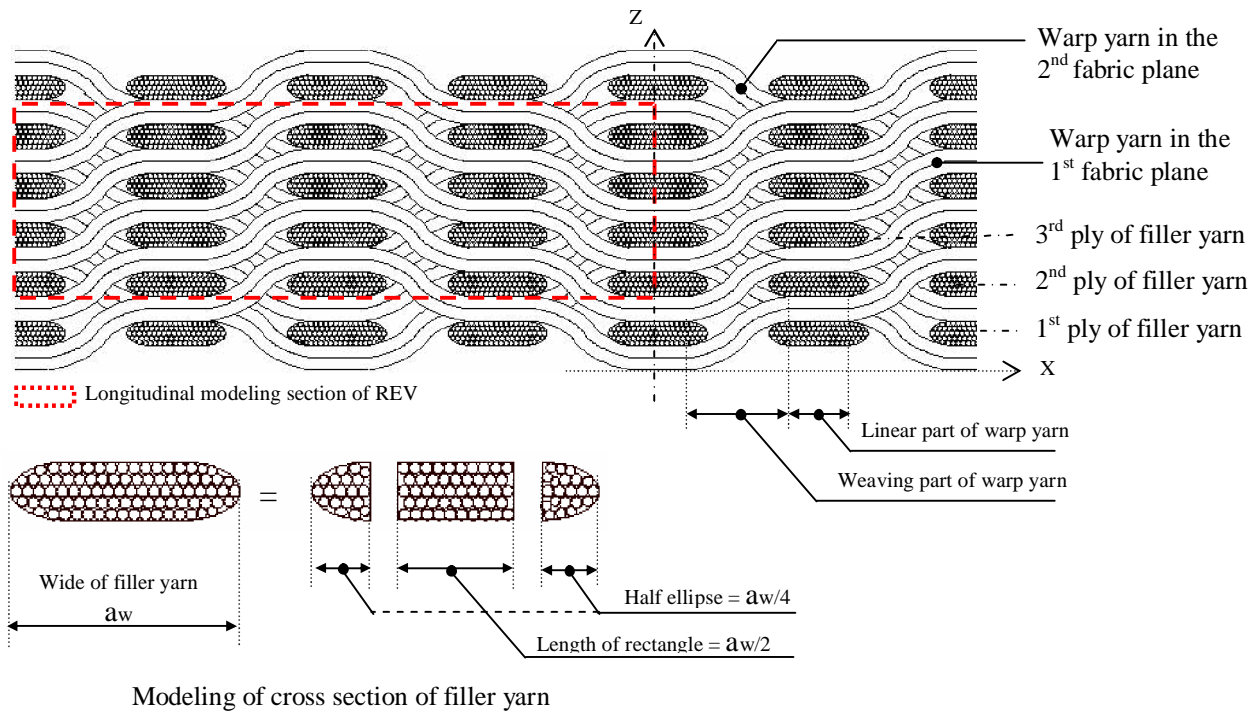


Figure 2: Modeling of longitudinal section of REV by showing the two longitudinal plans transparency of internal design of angle interlock 2.5D fabric

3.2. Modeling of transversal section of REV

Three geometrical modeling of transversal section are proposed. They are presented by case 1, case 2 and case 3 in figure 3. In all cases, the filler yarns are modeled by an undulated profile and the cross section of warp yarn is modeled by an ellipse. The dimension of width of cross section of warp yarn in each case is proposed in order to conserve a constant volume of REV. The pitch distance between the neighboring warp yarns is different in each case. The principal detail between each case is the position of cross section of warp yarn. In case 1, we consider the warp yarn with shift in the direction of 'xy' plane. In case 2, which is closed to reality, we consider the warp yarn in shift position in two directions 'xy' and 'xz' plane. In case 3, the warp yarns are aligned well in the 'yz' plane without shift.

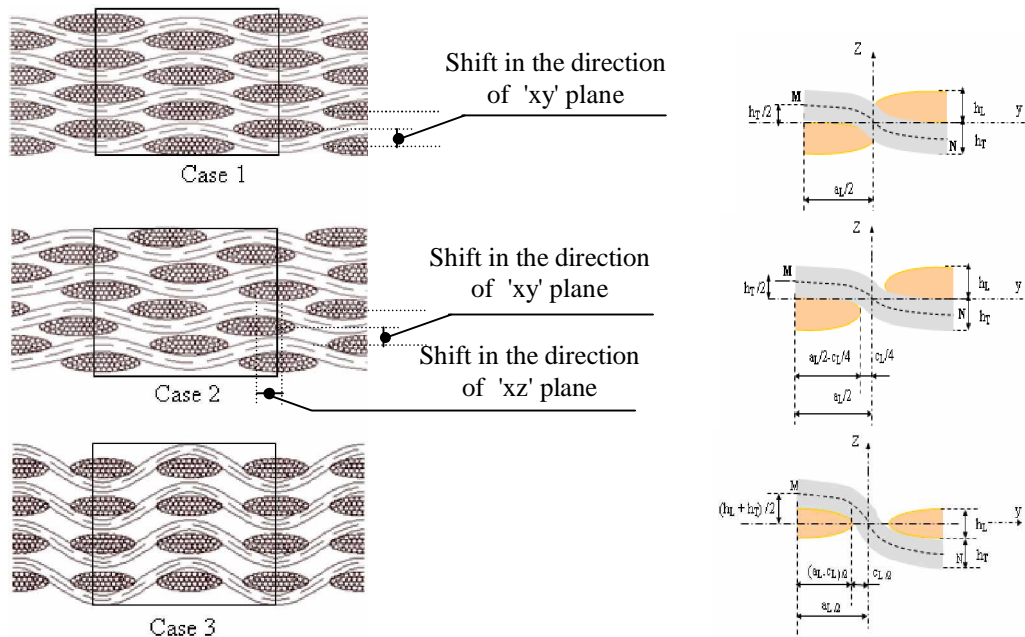


Figure 3: Three modeling cases of transversal section of REV

4. Analytical modeling of homogenization

The REV is divided according to its components, warp or fill yarns and resin. The analytical modeling applied to the REV is a model of homogeneity by summing the average stiffness of each component of basic cell. This homogeneity consists of determining the global matrix rigidity starting from the basic rigidities of the components $C_{ij,k}$ according to Eq.(1). Where n is the number of component equal to three in our application and V_k is the volume of each component.

$$C_{ij,Global} = \frac{1}{V_i} \sum_{k=1}^n V_k \cdot C'_{ij,k} \quad ; \text{ for: } i=1,\dots,6 \text{ and } j=1,\dots,6 \quad (1)$$

To be able to apply the model of homogenization to its expression (1), the analytical modeling generates the calculation of the matrix of rigidity $C'_{ij,k}$. If the component corresponding to a reinforcement, the matrix of rigidity $C_{ij,k}$ expressed in its own reference, is transformed in the global reference $C'_{ij,k}$ by the application of Eq.(2).

$$[C'_{ij,k}] = [T_\sigma]^t \cdot [C_{ij,k}] \cdot [T_\epsilon] \quad (2)$$

Where, $[T_\sigma]^t$ is the transposed matrix of basic change of stiffness function of the orientation of fibers and $[T_\epsilon]$ is the basic strain matrix also function of the orientation of fibers.

The 3D elastic properties represented by the 9 modules of engineer: $E_1, E_2, E_3, G_{12}, G_{13}, G_{23}, \nu_{12}, \nu_{13}, \nu_{23}$, are determined by the orthotropic global matrix rigidity (Berthelot, 1999).

The analytic elastic modeling is also determining the ultimate properties in particular in uni-axial tension. It's then possible to determine the state of stress in each component by assuming the continuity of the strains. A 3D rupture criterion of Tsai-Wu type which takes into account the three-dimensional effect of the texture of fiber is then applied to each increment of loading. The tensorial of the criterion is given in Eq.(3). In case of orthotropic structure, subjected in 3D stress state, the Eq.(3) is written by Eq.(4).

$$F_i \cdot \bar{\sigma}_i + F_{ij} \cdot \bar{\sigma}_i \cdot \bar{\sigma}_j = 1 \quad ; \text{ for } i,j = 1 \dots 6 \quad (3)$$

$$F_1 \cdot \sigma_1 + F_2 \cdot \sigma_2 + F_3 \cdot \sigma_3 + 2F_{12} \cdot \sigma_1 \cdot \sigma_2 + 2F_{13} \cdot \sigma_1 \cdot \sigma_3 + 2F_{23} \cdot \sigma_2 \cdot \sigma_3 + F_{11} \cdot \sigma_1^2 + F_{22} \cdot \sigma_2^2 + F_{33} \cdot \sigma_3^2 + F_{44} \cdot \sigma_4^2 + F_{55} \cdot \sigma_5^2 + F_{66} \cdot \sigma_6^2 = 1 \quad (4)$$

The linear terms F_i and F_{ii} of this expression for fibers are determined by ultimate stresses in compression, tension and shearing tests. The ultimate stresses in tension, compression and shearing of fiber, are required according to the literature. For T300J the value of X^+, X^-, Y^+ and S are those given by the company (SOFICAR, 2004). The ultimate properties of resin are required according to (Hexcel.composite, 2004). In fact, the complexity to using such a criterion, resides in the determination of the interactions coefficients F_{ij} . As regards this study, the coefficients are calculated by using experimental results established by (Khelil, 1993), from which predict the other ultimate stresses Y^-, Z^+, Z^-, R and Q. The table 1 presents the limits properties of 2D composite T300J/M6 at 0.6 volume fraction. Of these values, the 3D limits properties of yarns are required from adjustable equivalence with volume fraction in yarns. The 3D rupture criterion is able to determine the local states of stresses for a macroscopic level. At every increment of load, the 3D criterion of Tsai is applied to the local state of stress for each yarn. The composite is considered in the state of failure, when the criterion of rupture is reached for the two types of yarn. We considered also in this model that, when a component (resin or yarn) fails during loading, we neglect its strength in all direction by imposing its matrix rigidity equal to zero.

Table 1: Limits properties of 2D composite at 0.6 volume fraction composed by T300 J and M6 resin

	3D limit stiffness of component yarn and resin								
	Limit stiffness of tension			Limit stiffness of compression			Limit stiffness of shear		
	(GPa)			(GPa)			(GPa)		
X^+	Y^+	Z^+	X^-	Y^-	Z^-	Plan xy S	Plan xz R	Plan yz Q	
Composite 2D T300J, $V_f=0.6$	2.050 ^a	0.080 ^a	0.1101 ^b	1.570 ^a	0.3261 ^b	0.3571 ^b	0.098 ^a	1.3007 ^b	0.0728 ^b
Resin RTM6	0.075 ^c			0.160 ^c			0.050 ^c		

^a Data base of fiber (SOFICAR, 2004), ^b Study of (Khelil, 1993), ^c Data base of resin (Hexcel.composite, 2004)

5. Damage and rupture processes

Concerning the experimental part, the behavior of materials was investigated under tensile loading in the weft direction. The materials are prepared for tests, in rectangular form with constant section in addition of heels and instrumented by one bidirectional gauge. The damage and the failure mechanisms were identified by microscope observations. It's summarized by five stages: 1- Release of ruptures and shearing the end of filler yarn. 2- Propagation of rupture through the trajectories of interface warp/filler yarn, followed by shearing rupture of resin blocks. 3- Interface rupture of warp or filler yarn/resin by surrounding warp yarns, followed by longitudinal rupture of filler yarns. 4- Longitudinal damage of filler yarns which appear first, in the places with stronger slop. 5- Multiplication of longitudinal ruptures of warp yarns. The microscopic observations accompanied by a detection of the damage by acoustic emission (AE) are compared with their identification attributed to stages of amplitude established by (Barré and Benzeggagh, 1994) shows in figure 4. The analysis of results is based at the same time on the evolution of the load and the cumulative acoustic emission (AE) represented by the distribution the number of events in each stage of amplitude presented in figure 4. These results show that the microcracks in the matrix, multiplied along the test by preserving a constant sum of events. For the rupture of fiber, they appear only in second phase of test, the distribution of the group of dots of the number of events follows a Gaussian curve.

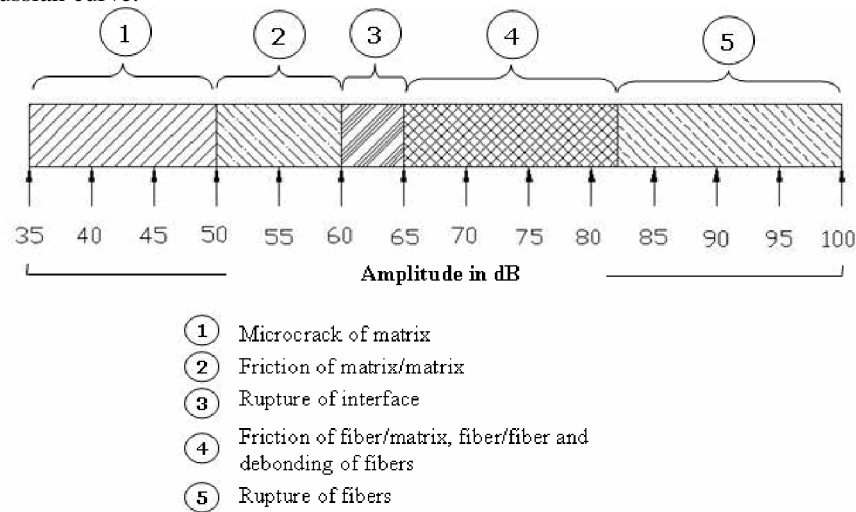


Figure 4: Attributed amplitude stages to different types of damage (Barré and Benzeggagh, 1994)

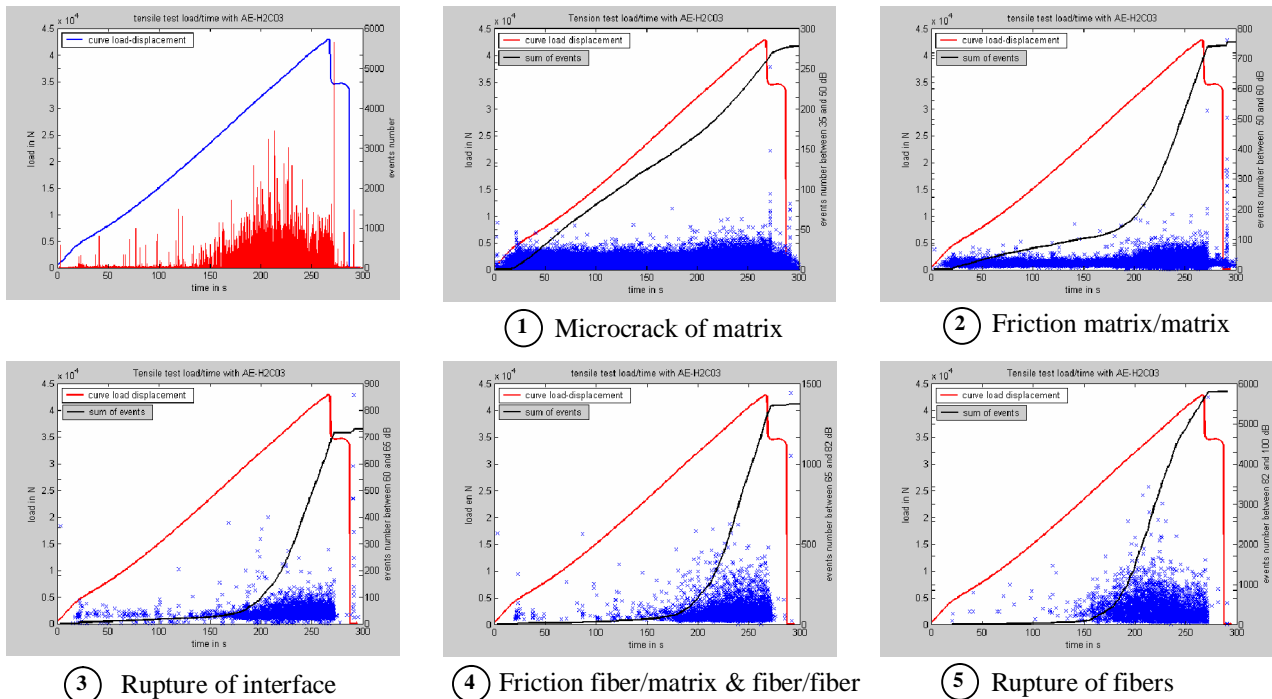


Figure 5: Evolution of load and her corresponding AE results distributed by stage of amplitude of tensile test in weft direction

6. Results and discussion

For the total fiber rates with 38% and for the proportions of 35% and 65% respectively in warp and fill yarn, the table 2 presents the elastic mechanical properties predicted by analytical model for yarns in each case of REV. The table 3 presents the 3D elastic mechanical properties for the composite interlock predicted by analytical model for each case of REV. With respect to experimental results, the case 2, predict better the longitudinal elastic module in weft direction. For the longitudinal elastic module in fill direction, all cases give a less value with respect to experimental results. The ultimate properties in tensile test in weft direction are also predicted by the analytical model. The state of stress in each component is also estimated by the analytical model by assuming the continuity of the strains. The table 4 shows the comparative results of ultimate properties between the experimental studies and the analytical model predicted for each case of REV. For all tests, the bidirectional gauge is released, so the limit strain is not identified. On the other hand, the rupture stress predicted by all the cases is stronger then the experimental result. This different can be attached to the criterion rupture of resin which is never attained due to the assumption of continuity of strain. We signaled that the limit strain of resin Epoxy M6 and the fiber T300J is respectively 3.4% and 1.8%. The figure 6 presents the stress-strain diagrams of tensile test in weft direction obtained by analytical and experimental results. We also show the subestimation of ultimate properties in all cases of REV.

Table 2: Elastic properties of yarns in each analytical modeling of VER

Geometric modeling	Type of yarns	Mechanical properties of yarns						
		V_f	E_L (GPa)	$E_T = E_Z$ (GPa)	$G_{LT} = G_{LZ}$ (GPa)	G_{TZ} (GPa)	ν_{LT}	ν_{TZ}
VER case 1	warp	0.6683	154.68	12.82	5.09	4.38	0.32	0.46
	filler	0.5540	128.71	9.26	3.59	3.14	0.32	0.47
VER case 2	warp	0.7387	170.66	16.44	6.60	5.64	0.31	0.46
	filler	0.5540	128.71	9.26	3.59	3.14	0.32	0.47
VER case 3	warp	0.8256	190.39	24.48	9.96	8.46	0.31	0.45
	filler	0.5527	128.42	9.23	3.58	3.13	0.32	0.47

Table 3: Elastic properties of the Interlock: comparison of results between the three cases and experimental

	E_1 (GPa)	E_2 (GPa)	E_3 (GPa)	ν_{12}	ν_{13}	ν_{23}	G_{12} (GPa)	G_{13} (GPa)	G_{23} (GPa)
Case1	53.410	63.410	12.783	0.062	0.625	0,220	3.844	6.432	4.717
Case2	53.433	62.415	13.421	0.064	0.608	0.237	4.111	6.657	4.551
Case3	54.849	62.868	16.034	0.075	0.565	0.249	5.003	7.556	7.253
Experimental	53.71±0.39	67.02±5.82	-	0.080±0,009	-	-	-	-	-

Table 4: Comparative of ultimate properties between experimental study and analytical model

	Strain and stress at failure for tensile test in the weft direction			
	warp yarn		Fill yarn	
	Rupture stress σ_{xx} [MPa]	Limit strain ϵ_{xx} %	Rupture stress σ_{xx} [MPa]	Limit strain ϵ_{xx} %
Case1	530	1.49	400	0.97
Case2	560	1.45	380	0.83
Case3	550	1.61	460	1.18
Experimental	392.01±26.63*	N.I		

* The failure of composite is produced close to the heels

N.I: not identify, release of the gauge.

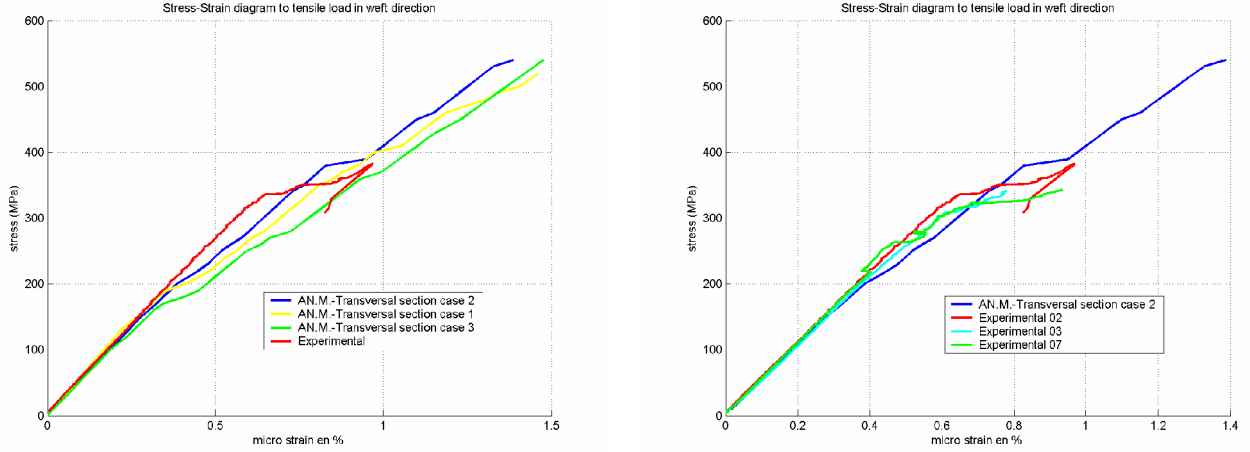


Figure 6: Stress-strain diagram of tension load in weft direction between analytical model and experimental

For the prediction of the ultimate properties, the rupture of the tested composite on the level of heels can be a cause for the large difference between the experimental and the analytical results. However, we proposed in this study an adjustment on the analytical model to estimate better these ultimate properties.

To reduce these properties, we proposed to deteriorate the matrix rigidity of resin while preserving for the yarn failure his strength (function of fiber's direction) in the directions other than direction of loading presented in table 5. This analytical model with deterioration of matrix rigidity, are noted by AMDR.

Table 5: Analytical model proposed for deteriorated the matrix rigidity of failure yarns in tensile test in weft direction

Warp yarn	Fill yarn
$C_{ij} = 0 \quad \text{for } i \neq j ; i, j = 1 \dots 6$	$C_{ij} = 0 \quad \text{for } i \neq j ; i, j = 1 \dots 6$
$C_{ii} = 0 \quad \text{for } i = 1 \text{ and } i = 4 \dots 6$	$C_{ii} = 0 \quad \text{for } i = 2 \text{ and } i = 4 \dots 6$
$C_{22 \text{ failure yarn}} = C_{22 \text{ initial yarn}}$	$C_{11 \text{ failure yarn}} = C_{11 \text{ initial yarn}}$
$C_{33 \text{ failure yarn}} = C_{33 \text{ initial yarn}}$	$C_{33 \text{ failure yarn}} = C_{33 \text{ initial yarn}}$

The studies of AE results in stage 35-50 dB, shows the multiplication of rupture in matrix with increment load. The sum of events is generated by the same compliance of the curve load-displacement. We proposed in Analytical Model Deteriorate Rigidity (AMDR) the deterioration of the matrix rigidity of resin by a compliance with the criterion rupture of fiber of filler yarns presented by Eq.(5) and Eq.(6).

For each increment of loading, the Eq.(5) is calculated.

$$F_i \cdot \bar{\sigma}_i + F_{ij} \cdot \bar{\sigma}_i \cdot \bar{\sigma}_j = C_{r \text{ fill yarn}} \quad ; \text{ for } : i, j = 1 \dots 6 \quad (5)$$

Where, $C_{r \text{ warp yarn}}$ presents a value of application of Tsai criterion rupture of warp yarn in the horizontal direction.

This number should be < 1 .

The matrix rigidity of resin $C_{ij \text{ re sin}}$ is calculated for each loading by Eq.(6).

$$C_{ij \text{ re sin of } (k+1) \text{ load}} = (1 - \eta \cdot C_{r \text{ warp yarn}}) \cdot C_{ij \text{ re sin of } (k) \text{ load}} \quad ; \text{ for } : i, j = 1 \dots 6 \quad (6)$$

Where, $\eta = 3.5$ is a multiplicative number, function of interlock fabric. This number is been determined by statistical study of the density of repartition dots between the stage 35-50 dB (microcrack matrix) and the stage 82-100 dB (rupture fiber) for the number of events and dissipated energy. The figure 7, shows the stress-strain diagram between

experimental and AMDR results. The AMDR predicts for the failure stress 420 MPa for 560 MPa predicted by the simple analytical model and 390.01 MPa given by experimental studies.

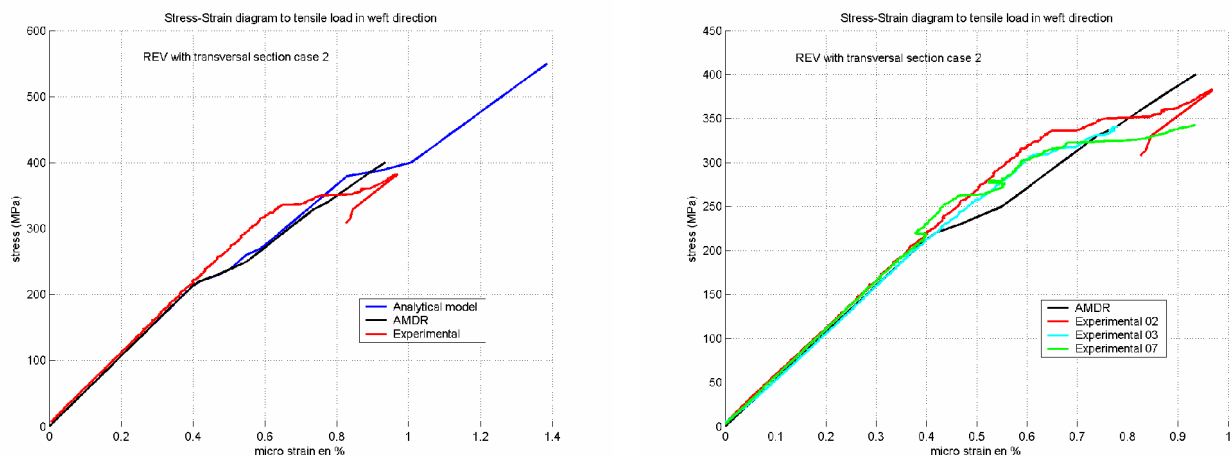


Figure 7: Stress-strain diagram of tension load in weft direction between AMDR and experimental

7. Conclusion

In this study we are highlighting the effects of internal geometry on the mechanical properties of the composite CFRP by applying an analytical model. The REV whose transversal section is modeled by taking into account the shift of warp yarns in the 'xy' and 'xz' planes estimate better the elastic mechanical properties. This REV has the most complex internal geometry among the other two. The predicted stress-strain curve correlated well with experimental curve in particularly in the first part of loading. In the next step, for the ultimate properties, we should test another type of interlock 2.5D (CRFP) to confirm the necessity to deteriorate the matrix rigidity of resin and the utility of the application of the AMDR.

References

- Aboura, Z., Benzeggagh, M. L., Billaut, F. and Dambrine, B.** (1995). Mode I interlaminar Failure Stitched Textile Composite Materials: Predictive proposal of Reinforcement Model. *10th International Conference of Composite Materials. ICCM10 Vancouver.*
- Aboura, Z., El Hage, C., Younés, R., Benzeggagh, M. L. and Zoater, M.** (2005). Prédiction du comportement élastique endommageable de matériaux composites à renfort orthogonal 3D. *17ème Congrès Français de Mécanique. Troyes, septembre 2005.*
- Barré, S. and Benzeggagh, M. L.** (1994). On the use of acoustic emission to investigate damage mechanisms in glass-fibre-reinforced polypropylene. *Composites Science and Technology* **52**, 369-376.
- Berthelot, J. M.** (1999). Matériaux composites: Comportement mécanique et analyse des structures. *Edition: TEC&DOC. 3e édition.*
- El Hage, C., Younés, R., Aboura, Z., Benzeggagh, M. L. and Zoater, M.** (2005). Modélisation analytique et numérique des caractéristiques mécaniques d'un composite à renfort carbone 3D orthogonal. *14ème Journées Nationales sur les Composites. JNC14 Compiègne, France. Compte rendus des JNC14, volume 2, 699-708.*
- Hexcel.composite.** (2004). Référence:société Hexcel composite. <http://www.Hexcel.com>.
- Khelil, K.** (1993). Evaluation expérimentale d'un critère de rupture tensoriel polynomial tridimensionnel pour matériaux composites. *. Thèse de doctorat de l'Université de Compiègne.*
- Scida, D., Aboura, Z., Benzeggagh, M. L. and Bocherens, E.** (1998). Prediction of the elastic behaviour of hybrid and non-hybrid woven composites. *Composites Science and Technology* **57**, 1727-1740.
- SOFICAR.** (2004). Référence: Société de fibres de carbone. <http://www.soficar-carbon.com>.